# Diffusion behavior of helium in titanium and the effect of grain boundaries revealed by molecular dynamics simulation*

Gui-Jun Cheng(程贵钧)[1], Bao-Qin Fu(付宝勤)[2,†], Qing Hou(侯氢)[2], Xiao-Song Zhou(周晓松)[1], and Jun Wang(汪俊)[2]

[1] *Institute of Nuclear Physics and Chemistry, China Academy of Engineering Physics, Mianyang* 621900, *China*

[2] *Key Laboratory for Radiation Physics and Technology, Institute of Nuclear Science and Technology, Sichuan University, Chengdu* 610065, *China*

(Received 29 January 2016; revised manuscript received 15 March 2016; published online 1 June 2016)

The microstructures of titanium (Ti), an attractive tritium (T) storage material, will affect the evolution process of the retained helium (He). Understanding the diffusion behavior of He at the atomic scale is crucial for the mechanism of material degradation. The novel diffusion behavior of He has been reported by molecular dynamics (MD) simulation for the bulk hcp-Ti system and the system with grain boundary (GB). It is observed that the diffusion of He in the bulk hcp-Ti is significantly anisotropic (the diffusion coefficient of the [0001] direction is higher than that of the basal plane), as represented by the different migration energies. Different from convention, the GB accelerates the diffusion of He in one direction but not in the other. It is observed that a twin boundary (TB) can serve as an effective trapped region for He. The TB accelerates diffusion of He in the direction perpendicular to the twinning direction (TD), while it decelerates the diffusion in the TD. This finding is attributable to the change of diffusion path caused by the distortion of the local favorable site for He and the change of its number in the TB region.

**Keywords:** diffusion, grain boundary, helium and titanium, molecular dynamics

**PACS:** 66.30.J–, 61.72.Mm, 66.30.–h, 61.72.–y **DOI:** 10.1088/1674-1056/25/7/076602

## 1. Introduction

Hydrogen (H) storage materials have been used for the storage, purification, and compression of tritium (T) and the separation of hydrogen isotopes (including H, deuterium (D) and T), which is one of the necessary steps for achieving the controlled thermonuclear reaction. Helium (He), introduced by direct implantation or produced by T decays with a 12.32 year half-life,[1,2] is retained in the hydrogen storage materials, although He is normally insoluble in such materials. The retained He atoms, driven by temperature, move randomly in the substrate until they become trapped in sites, such as vacancy, dislocation, grain boundary (GB), and He cluster.[3] The accumulation of He atoms results in the formation of bubbles,[4,5] and further evolution may produce void swelling, embrittlement, surface roughening, blisters, and material damage. The interaction between He and metal crystals is of considerable interest, and a number of efforts have been dedicated to address the microscopic mechanisms of the evolution process.[6–8] The evolution process is highly complex and may alter the mechanical and thermodynamic properties of substrate materials. Because diffusion of He atoms in the substrate materials is essential for the microscopic mechanisms of the evolution process, we will focus on the diffusion behavior of He in hydrogen storage materials.

Titanium (Ti), because of its low cost and key advantages, such as stability in air, high storage capacity, low storage pressure, and acceptable He retention rate,[9] has long been considered to be a good candidate for the long-term storage of T. At low temperature, the stable phase of Ti is a hexagonal close-packed (hcp) structure,[10,11] which is also the initial phase of Ti with low H content according to the Ti–H phase diagram.[12] As for hcp-Ti, deformation twinning plays an important role in the plastic deformation,[13–16] and twinning occurs predominantly in the $\{10\bar{1}2\}\langle\bar{1}011\rangle$ system (where $\{10\bar{1}2\}$ is the twinning plane and $\langle\bar{1}011\rangle$ is the twinning direction in the twinning plane), although $\{11\bar{2}1\}\langle11\bar{2}\bar{6}\rangle$, $\{11\bar{2}2\}\langle11\bar{2}\bar{3}\rangle$, and $\{10\bar{1}1\}\langle10\bar{1}2\rangle$ have also been observed.[14,16,17] Thus, twin boundaries (TB), the simplest and important GB, usually exist in the engineering materials. The existence of GBs and other crystal defects will affect the evolution behavior of He in polycrystalline Ti. In addition, the presence of GBs is considered to promote the resistance to radiation damage.[18–20] To understand comprehensively the effect of GB on the diffusion behavior of He, it is critical to obtain detailed descriptions of the fundamental atomistic processes, which can be studied by molecular dynamics (MD) simulation.

As the key theoretical tool for understanding how microstructural effects in materials occur at the atomistic level, MD simulations have been used to investigate collective phenomena, such as transport phenomena, plastic deformation, and radiation damage. There have been a number of MD simu-

*Project supported by the National Natural Science Foundation of China (Grant No. 51501119), the Scientific Research Starting Foundation for Younger Teachers of Sichuan University, China (Grant No. 2015SCU11058), the National Magnetic Confinement Fusion Science Program of China (Grant No. 2013GB109002), and the Cooperative Research Project "Research of Diffusion Behaviour of He in Grain Boundary of HCP-Titanium", China.

†Corresponding author. E-mail: bqfu@scu.edu.cn

© 2016 Chinese Physical Society and IOP Publishing Ltd 

lations that consider the interaction between He and Ti.[7,21–23] The He–Ti interatomic potential, constructed by Wang *et al.*,[7] can reproduce the clustering process of He in Ti. It is found that He clusters at a certain size tend to grow further through the relief of their pressure resulting from the emission of defects.[21] Chen *et al.*[22,23] first studied the diffusion behavior of He in Ti and found that the diffusion of $He_n$ ($n = 1$, 2, and 3) is anisotropic and He-dimer migrates more quickly than single He. However, these studies are still preliminary, and further research in this field is warranted, especially the effect of GBs.

The purpose of this paper is to study the diffusion behavior of He in Ti and the effect of GBs using MD simulations. The rest of this paper is organized as follows. In Section 2, we will describe the interatomic potentials, the creation of the simulation box without and with a TB, and the other details of the MD simulation. In Section 3, we will present the simulation results and discuss the diffusion behavior of He in Ti without and with a TB.

## 2. Simulation details

### 2.1. Interatomic potential

The interatomic potential, which is used to calculate the atomic forces in each time step, is the key ingredient of the MD simulation. In recent years, there have been many published interatomic potentials[24–28] used to describe the Ti-Ti interaction. In this work, two Ti–Ti potentials are used: one is the empirical tight-binding potential produced by Cleri and Rosato[28] (abbreviated as Cleri1993), and the other is an embedded atom method (EAM) potential produced by Zope and Mishin[26] (abbreviated as Zope2003). Before the formal simulation, the equilibrium cell parameters ($a$ and $c$) should first be calculated for various potentials; the results of such calculations are shown in Table 1. For comparison, we also present the results calculated with another EAM-type potential produced by Zhou[25] (Zhou2004). The Zope2003 potential clearly gives more accurate predictions for the cell parameters and cohesive energy than the other two potentials, based on the comparison with the experimental data.[29,30] The ratio of cell parameters $c/a$ is critical for the physical performance of a hcp metal,[11,27,31] and the experimental value of hcp-Ti has a large discrepancy from the ideal value 1.633, which will affect its microstructure. Therefore, in the following simulations, we mainly concentrate on Zope2003, with results from Cleri1993 also being quoted when relevant.

An EXP6 model, produced by Young *et al.*,[32] was applied to describe the He–He interaction, because it has been widely used to study He effects in solid materials.[8,33–35] The expression for the He–He potential energy ($V_{\mathrm{He-He}}$) can be described by

$$V_{\mathrm{He-He}}(r) = \varepsilon\left[6\mathrm{e}^{a(1-r/r^*)} - a\left(r^*/r\right)^6\right]/(a-6), \qquad (1)$$

where the potential parameters $\varepsilon$, $a$, and $r^*$ are 0.00093 eV, 13.1, and 2.97 Å,[32] respectively. As was performed earlier for tungsten's potential,[36] the He potential has also been modified by connecting the ZBL universal potential[37] to ensure the short range reliability.

**Table 1.** Equilibrium cell parameters ($a$, $c$, and $c/a$) and cohesive energy ($E$) of Ti predicted by three interatomic potentials (Cleri1993,[28] Zhou2004,[25] and Zope2003[26]) in comparison to the experimental data.[29,30]

| | Cleri1993 | Zhou2004 | Zope2003 | Expt. |
|---|---|---|---|---|
| $a$/Å | 2.810 | 2.939 | 2.956 | 2.951 |
| $c$/Å | 4.586 | 4.769 | 4.684 | 4.684 |
| $c/a$ | 1.632 | 1.623 | 1.585 | 1.587 |
| $E$/(eV/atom) | –4.855 | –4.870 | –4.850 | –4.850 |

Regarding the Ti–He interaction, there are few published interatomic potentials. Only a pair-wise potential, in the form of the Lennard–Jones potential fitted with the first-principles calculation,[7] has been used in our recent studies,[21,23,35] where the implementation is described in detail. The Ti–He potential energy ($V_{\mathrm{Ti-He}}$) is written as

$$V_{\mathrm{Ti-He}}(r) = \mu\left(r_0/r\right)^{\alpha} - \lambda\left(r_0/r\right)^{\beta}, \qquad (2)$$

where the potential parameters $\mu$, $\lambda$, $r_0$, $\alpha$, and $\beta$ are 0.026 eV, 0.084 eV, 4.73 Å, 4.35, and 1.4,[21] respectively. Based on the above potentials, the research on diffusion behavior of He in Ti and GB's effects has been performed using MD simulations.

### 2.2. Simulation setup

All MD simulations were performed using MDPSCU, an MD package that can be run on multiple graphic processing units (GPUs) for parallel computation.[38] The MD simulator has been modified by Fu through the addition of some functional modules, such as box creation.

In an MD simulation, atomic information (e.g., positions and velocities), generated by integrating the classical equations of motion, can be available to analyze the evolution process in detail. The Velocity–Verlet algorithm, proposed by Swope *et al.*,[39] has been used to integrate Newton's equations of motion for atoms. For efficiency, the simulation box should be kept as small as possible. For the case of bulk Ti (without TB), the lengths of $x$, $y$, and $z$ axes for the simulation box are $10a$, $10\sqrt{3}a$, and $10c$, respectively, and the $x$, $y$, and $z$ axes are along $[2\bar{1}\bar{1}0]$, $[01\bar{1}0]$, and [0001] directions, respectively. Finite-size effects are dealt with using periodic boundary conditions (PBCs) along all the $x$, $y$, and $z$ axes. The simulation box contains 4000 Ti atoms, and He atoms are added at random locations more than 0.5 Å away from the closest Ti atom in the box before simulation. Each calculation is executed one time section after another. In the first time section, the time step ($t$) is automatically adapted to minimize the maximum displacement of atoms in the evolution. Next, the He atoms will move to the nearest favorable interstitial site by "quenching" the system, i.e., the velocity of atom $i$ will be cancelled

when the product $F_i(t) \cdot v_i(t)$ of force ($F$) and velocity ($v$) is negative (quenching MD[40]). In the next time section, the fixed time step is 1 fs (femtosecond), and the simulation boxes are thermalised to a given temperature ranging from 300 K to 1200 K with sufficient time steps (total time is 20000 fs) to bring them to thermal equilibrium. Thermalisation of a simulation box is conducted by assigning the atoms in the box with velocities generated by the Monte Carlo (MC) sampling of the Maxwell distribution of atom velocity. In the next time section, a micro-canonical ensemble is performed to study the diffusion behavior of He; the total time is 180000 fs, with a fixed time step of 1 fs. Finally, quenching MD is performed to obtain the last atomic configurations of the simulation boxes. In the whole simulation, the states of the simulation boxes were recorded every 5000 fs. For each temperature, 500 independent replicas with different initial states were executed for the ensemble average method.

We chose $\{10\bar{1}2\}$ TB as a typical representative to study the diffusion behavior of He in the GB region. The simulation boxes with TB were first constructed as illustrated in Fig. 1. A TB, which exists in the middle of the box, is the interface between the upper and lower grains with mirror symmetrical crystallographic orientations. For $\{10\bar{1}2\}$ TB, the $x$ direction of the simulation box is $\boldsymbol{a}_1 = \boldsymbol{a}_2 = [\bar{1}011] = [\bar{2}\bar{1}1]$ (three indices) $= -3a\boldsymbol{i}/2 - \sqrt{3}a\boldsymbol{j}/2 + c\boldsymbol{k}$, the $y$ direction is $\boldsymbol{b}_1 = \boldsymbol{b}_2 = [1\bar{2}10]/3 = [0\bar{1}0] = a\boldsymbol{i}/2 - \sqrt{3}a\boldsymbol{j}/2$, the $z$ direction of the upper grain is $\boldsymbol{c}_2 = \sqrt{3}c\boldsymbol{i}/2 + c\boldsymbol{j}/2 + \sqrt{3}a\boldsymbol{k}$ and that of the lower grain is $\boldsymbol{c}_1 = -\boldsymbol{c}_2$ (where $\boldsymbol{i}$, $\boldsymbol{j}$, and $\boldsymbol{k}$ represent the three axes of the Cartesian coordinate system). For the case of TB, PBCs have been used only in the $x$ and $y$ directions; thus, the top and bottom regions of the simulation box are a vacuum. The simulation box size is 34.7 Å $\times$29.56$\times$152.06 Å, including 6500 Ti atoms from one eighth of the $z$ dimension ($L_{z/8}$) to seven eighths of the $z$ dimension ($L_{7z/8}$). The simulation box was first relaxed to minimize the potential energy using quenching MD (annealing). In the simulation, the atoms of the top and bottom five layers (ten single layers) are kept fixed in the perfect lattice sites. Figure 2 shows the atomic configuration (projection along the $y$ axis) of boxes before and after annealing. Because the hcp crystal structure has two atoms per lattice site, it can be observed that the two single layers, which are the symmetrical planes of the initial box with TB, converge into one layer as labelled by the dash green line. This finding is in agreement with the atomic configuration of TBs for some hcp metals observed experimentally with high-angle annular dark-field scanning transmission electron microscopy (HAADF-STEM) by Nie *et al.*[15] According to many trails, we find that any GBs in which a single layer is taken as the symmetrical plane are unstable. Next, He atoms are randomly

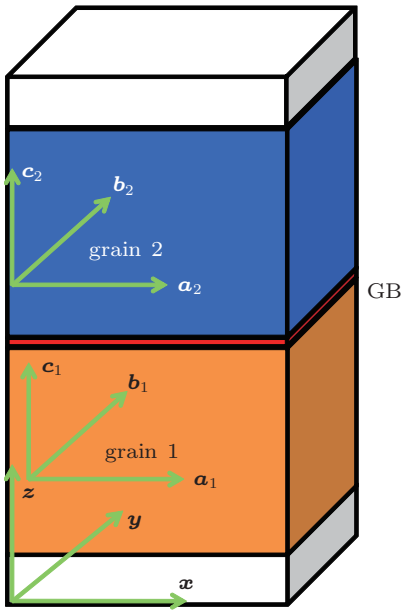



**Fig. 1.** (color online) Schematic representation of creation of simulation box with a GB. The lower grain (Grain 1) and the upper grain (Grain 2) with different crystallographic orientations ($\boldsymbol{a}_1$, $\boldsymbol{b}_1$, $\boldsymbol{c}_1$ and $\boldsymbol{a}_2$, $\boldsymbol{b}_2$, $\boldsymbol{c}_2$, respectively) are separated by the GB, which is the symmetrical plane denoted with the red layer. The top and bottom regions of the box are vacuums.

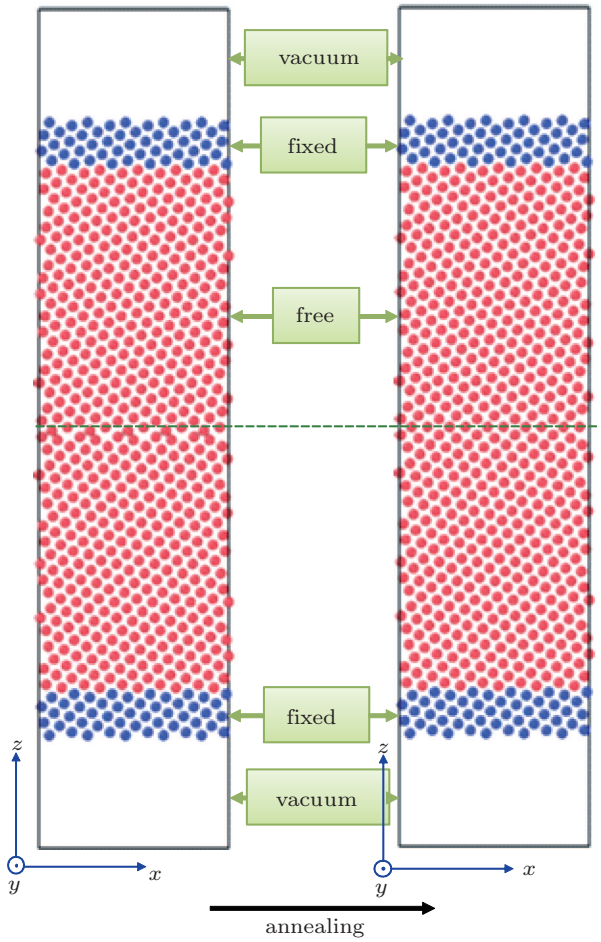



**Fig. 2.** (color online) Atomic configuration (projection along the $y$ axis) of boxes before (a) and after (b) annealing. The TB plane is underlined by the green dashed line. The red spheres represent free atoms and the blue spheres represent the fixed atoms.

added near the TB plane and placed at more than 0.5 Å away

from the closest Ti atom in the simulation box. The rest of the simulation details (temperature and box volume) for the case of TB are the same as those for the case of bulk-Ti.

## 3. Results and discussion

The diffusion coefficient ($D$) provides a more quantitative description on the diffusion features; the value of the diffusion coefficient can be obtained from the mean square displacements (MSD) according to the Einstein relation[41]

$$D = \lim_{t\to\infty} \frac{\langle |\boldsymbol{R}(t)|^2 \rangle}{2dt}, \tag{3}$$

where $t$ is the evolution time, $\boldsymbol{R}(t)$ is the displacement vector of the particle undergoing diffusion, $\langle |\boldsymbol{R}(t)|^2 \rangle$ is the ensemble-averaged MSD, and $d$ is the dimensionality of the space in which diffusion is occurring. To study the diffusion behavior of various crystallographic orientations, the diffusion coefficient $D_{\alpha\alpha}$ ($\alpha = x$, $y$, or $z$) along each of three axes ($x$, $y$, or $z$) can be deduced from the MSD of each axis,[42]

$$D_{\alpha\alpha} = \lim_{t\to\infty} \frac{\langle |R_\alpha(t)|^2 \rangle}{2t}, \tag{4}$$

where $R_\alpha(t)$ is the $\alpha$-th component of the displacement vector. Similarly, $D_{\alpha\beta}$ ($\alpha \neq \beta$) can be defined as

$$D_{\alpha\beta} = \lim_{t\to\infty} \frac{\langle R_\alpha(t) R_\beta(t) \rangle}{2t}. \tag{5}$$

This function is actually the correlation function between the $\alpha$-th component of velocity and the $\beta$-th component of displacement at $t = \infty$. Note that $D_{\alpha\beta}$ ($\alpha \neq \beta$) should be zero when the $\alpha$-th component of velocity has no effect on the $\beta$-th component of displacement; this condition is related to the random walk behavior of particles undergoing diffusion.[43] Combining the above two formulae, the matrix form of diffusion coefficient ($\boldsymbol{D}$) can be rewritten as

$$\boldsymbol{D} = \lim_{t\to\infty} \frac{\langle \boldsymbol{R}(t) \otimes \boldsymbol{R}(t) \rangle}{2t}. \tag{6}$$

## 4. Diffusion behavior of He in bulk-Ti

According to the above formulae, the diffusion coefficients at various temperatures can be deduced. Figure 3 shows the excellent linear correlation between the ensemble-averaged MSD of He atoms in bulk-Ti at each direction and the diffusion time at 900 K as an example of the calculation and analysis. The MSD in all directions increases linearly with time, and the slope of the curves obtained in the $z$ direction is larger than those for the $x$ and $y$ directions. This finding indicates that the diffusion of He in hcp-Ti is anisotropic and higher in the [0001] direction, which resembles the results of Chen *et al.*[23] The same or a similar phenomenon can also be found in the other temperatures. Note that the values of $D_{\alpha\beta}$ ($\alpha \neq \beta$) in such a coordinate system are all very small and close to zero.

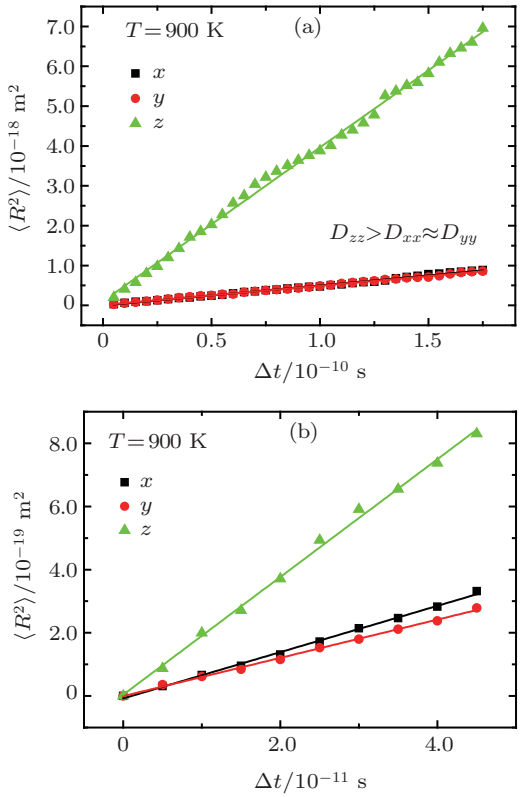



**Fig. 3.** (color online) Ensemble-averaged MSD ($\langle R^2 \rangle$) along the $x$, $y$, and $z$ axes as a function of time ($\Delta t$) at $T = 900$ K for He (a) and $He_2$ (b) in bulk Ti. The diffusion coefficient (half of the slope of the fitted line) is anisotropic ($D_{zz} > D_{xx} \approx D_{yy}$).

As presented in Fig. 4(a), it can be observed that the diffusion coefficient increases with the increase in temperature ($T$), which can be explained by Arrhenius law,

$$D = D_0 \exp\left(-\frac{\Delta E}{k_B T}\right), \tag{7}$$

where $D_0$ is a pre-exponential factor independent of the temperature, $\Delta E$ is the migration energy of He from one favorable interstitial site to the adjacent one, and $k_B$ is the Boltzmann constant. The linear relationship between $\ln D$ and $1/T$ shows that migration of He is a thermally activated process and accelerates with increasing temperatures, and Song *et al.* obtained a similar trend experimentally.[3] The values of $D_0$ and $\Delta E$ resulting from the fit of the data with the above formula are gathered in Table 2. The migration energies in the $x$ and $y$ directions ($\Delta E_x$ and $\Delta E_y$) are found to be close and higher than the migration energy in the $z$ direction ($\Delta E_z$), i.e., the significant anisotropy of diffusion is primarily caused by the quite different migration energies for He diffusion. The result is in disagreement with Chen's study; one possible explanation for the differences could be the lack of determination of the equilibrium cell parameters for the used potential.[23] For comparison, the similar simulation was performed using the Cleri1993 Ti–Ti potential because it was used by Chen;[23] the calculated results are shown in Fig. 4(b) and Table 2. It is also shown that

the diffusion is anisotropic, as also represented by the differences of migration energies of He. According to the Meyer–Neldel rule,[44] the pre-exponential factor increases with the increase in migration energy, which is consistent with our results for the two cases.

**Table 2.** Pre-exponential factor ($D_0$) and migration energy ($\Delta E$) along the $x$, $y$, and $z$ axes resulting from the fitted line in Fig. 4. The migration energy is anisotropic ($\Delta E_z < \Delta E_x \approx \Delta E_y$) and the pre-exponential factor increases with the increase of migration energy, following the Meyer–Neldel rule.[44]

| | Zope2003 | | | Cleri1993 | | |
|---|---|---|---|---|---|---|
| | $x$ | $y$ | $z$ | $x$ | $y$ | $z$ |
| $D_0/10^{-6}$ m$^2$/s | 3.534 | 4.287 | 1.759 | 0.870 | 0.744 | 0.547 |
| $\Delta E$/eV | 0.462 | 0.473 | 0.244 | 0.283 | 0.271 | 0.222 |

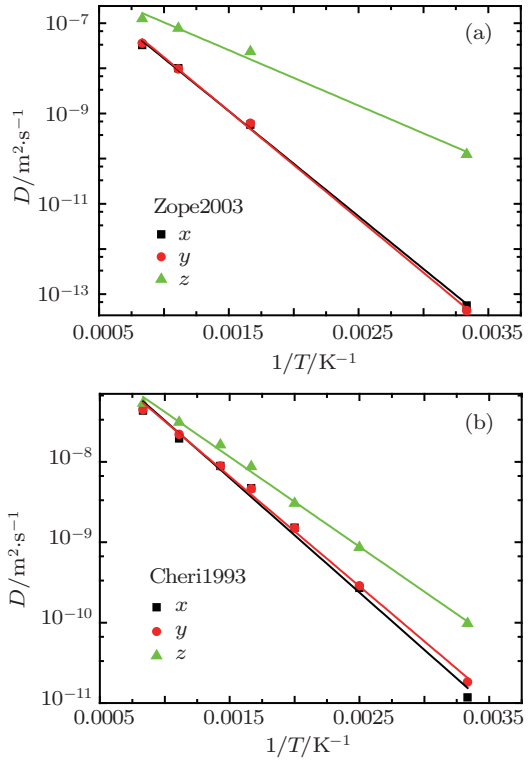



**Fig. 4.** (color online) Diffusion coefficient ($D$) along the $x$, $y$, and $z$ axes as a function of temperature ($T$) for He in bulk Ti. (a) Zope2003[26] and (b) Cleri1993[28] are used to describe the Ti–Ti interaction. These fitted lines can be explained by Arrhenius relation ($\ln D = \ln D_0 - \Delta E/k_B T$) and the migration energy ($\Delta E$) is also anisotropic ($\Delta E_z < \Delta E_x \approx \Delta E_y$).

In hcp-Ti, the He atoms are mobile via interstitial diffusion. Although there is no direct experimental evidence for where He atoms should be located, the moving He atoms are preferably located at the octahedral (O) site according to our MD simulation. It is found that the formation energy ($E_f = E(\mathrm{Ti}_n\mathrm{He}) - E(\mathrm{Ti}_n) - E(\mathrm{He})$) is 0.229 eV and the He atom migrates from one O site to another through an occasional jump. The jump direction of the moving He atom may be just along one of these directions, i.e., $\langle 0001 \rangle$ or $\langle 110 \rangle$, the jump distance of which is $c/2$ or $a$, respectively. The jump behaviors are significantly different for the He atoms diffusing in different directions, and the shorter jump distance may be one of the factors for the lowest migration energy along the $\langle 0001 \rangle$ direction. The diffusion anisotropy has been explained by the calculation results;[45] there exists a tube of low electron density along the $\langle 0001 \rangle$ direction and the activation energy of 0.34 eV calculated in Ref. [45] is close to our results. It is obvious that the velocity in the $\langle 0001 \rangle$ direction has no effect on the displacement in the basal plane, and vice versa. Due to the symmetry of the $\langle 11\bar{2}0 \rangle$ jump in the basal plane, the velocity in the $x$ direction has no effect on the $y$-th component of the displacement, and vice versa. Therefore, $D_{\alpha\beta}$ ($\alpha \neq \beta$) in such a coordinate system should be zero, consistent with our results.

The diffusion behavior of $\mathrm{He}_n$ ($n = 2$, 3, and 4) in bulk-Ti at 900 K has also been studied. It is found that these $\mathrm{He}_n$ atoms migrate without dissociation. In addition, the dissociation energy ($E_{nd} = nE_b(\mathrm{Ti}_m\mathrm{He}) - E_b(\mathrm{Ti}_m\mathrm{He}_n) - (n-1)E_b(\mathrm{Ti}_m)$, where $E_b(\mathrm{Ti}_m\mathrm{He}_n)$ is the total cohesive energy of the simulation box with $m$ Ti atoms and $n$ He atoms) are $E_{2d} = 0.75$ eV, $E_{3d} = 1.95$ eV, and $E_{4d} = 2.78$ eV. According to the Einstein relation, the diffusion coefficient of $\mathrm{He}_2$ can be deduced by the ensemble-averaged MSD of the mass centre of $\mathrm{He}_2$. As shown in Fig. 3(b), the diffusion of $\mathrm{He}_2$ is also anisotropic, as in the case of the single He atom. The evolutions of MSD of $\mathrm{He}_3$ and $\mathrm{He}_4$ are not plotted due to their lower jump frequency.

### 4.1. Diffusion behavior of He in TB region

Similar research on the diffusion behavior of He atoms in the TB region was conducted. Figure 5 shows the time evolution of MSD of He and $\mathrm{He}_2$ diffusion in the $y$ direction of the TB region at 600 K. Similar results, not shown here, are obtained at different temperatures. The evolution of MSD in the $x$ and $z$ directions is not plotted because the jump frequency of He in these two directions is too small. In addition, only when the jump steps are more than a certain value can we calculate the diffusion coefficient with MD simulation in a reasonable amount of time. For the $z$ direction, the $\mathrm{He}_n$ almost cannot jump outward from the TB region due to its absorption. For the case of He, at 600 K only three He atoms in the 500 independent simulations obviously escape from TB after the evolution of more than 200 ps. Therefore, the TB has high adsorption ability for the moving He atoms. Note that the escaped He atoms have not been counted into the ensemble average of MSD along the $y$ direction.

The $x$ axis of the simulation box for the case of TB is [011], which is the twinning shear direction of hcp crystal. As discussed above, the atoms in the symmetrical layers almost move into one plane, and the detailed movements of atoms in the TB region are shown in Fig. 6. After the quench relaxation of the TB region, the displacements of Ti atoms (parallel to the $y$ direction) are very small and almost negligible. However, the displacements (along the $x$ and $z$ directions) of Ti atoms near the TB are noticeable and decrease when running away from TB. The displacements of Ti atoms will affect the

He site occupation in the TB region and the detailed configuration of the local favorable site of He is also shown in Fig. 6. Through quenching the MD simulation for many boxes into which a He atom is randomly placed near TB, it is found that the He atoms prefer only a portion of the distorted octahedral sites, which will affect the jump path of He atoms along the $x$ direction. Therefore, the distortion of atoms in the TB region has a great influence on the diffusion of He atoms. The local favorable sites, marked by A (in the TB plane), B (approximately 1.27 Å from TB), and C (approximately 2.29 Å from TB) in Fig. 6, are decorated with a periodic distribution in the $x$ direction of the TB region. The formation energies of these local favorable sites are all approximately −2.5 eV and are less than that in the bulk Ti, i.e., the He atoms are soluble and trapped in the TB region.

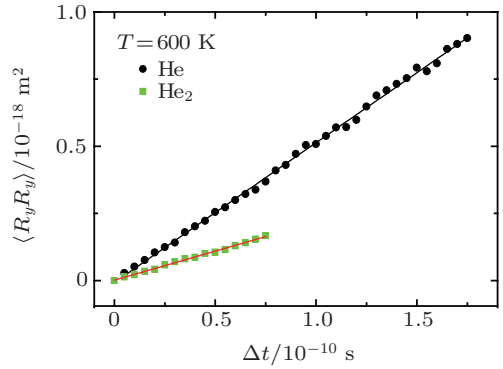



**Fig. 5.** (color online) Ensemble-averaged MSD ($\langle R_y R_y \rangle$) along the $\boldsymbol{y}$ direction as a function of time ($\Delta t$) at $T = 600$ K for He and $He_2$ in the TB region. The diffusion coefficient in the $y$ direction can be deduced as $1.04384\times10^{-8}$ m$^2$/s. The diffusion coefficients in $x$ and $z$ directions are too small to compute due to the rare jump event in these directions.

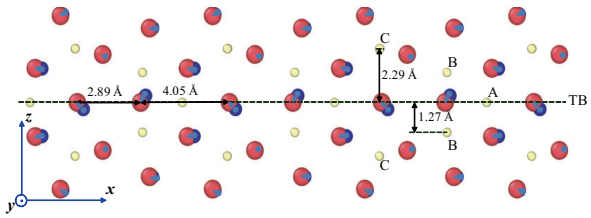



**Fig. 6.** (color online) The atomic structure (projection along the $y$ axis) of the TB region. The light blue arrows denote the displacements of Ti atoms before (represented by dark blue spheres) and after (represented by red spheres) quench relaxation. The TB plane is underlined by the green dashed line. The local favourable sites for He near the TB plane are denoted by the yellow spheres. These sites are all distorted octahedral sites.

As shown in Fig. 7, the formation energies of local favorable sites are calculated with quenching MD. It can be observed that the formation energies of the three sites (A, B, and C, as marked in Fig. 6) near the TB are minimal and increase when leaving TB, which implies attraction between He and TB. When the distance between He and TB is more than 5 Å, the formation energy is close to that in the bulk, i.e., the He can be regarded as desorbed. Therefore, for reliability, the He atoms more than 5 Å away from TB in the whole evolution will not be counted into the calculation of MSD for the case of TB. A study of the adsorption process of He in the TB region will be reported in a future publication. The excess ratio ($\chi = (d - d_{\text{perfect}})/d_{\text{perfect}}$) of the interplanar spacing of the twin boundary region was also calculated as shown in Fig. 7. Similar to the formation energies, the changes of interplanar spacing near TB are apparent.

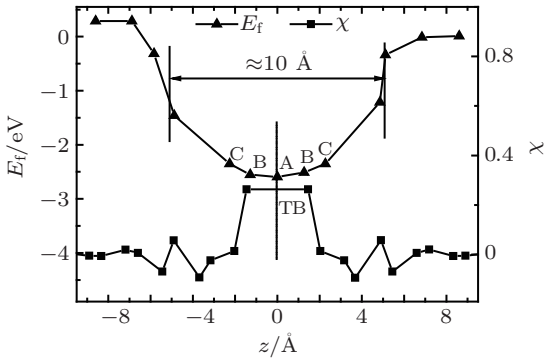



**Fig. 7.** The formation energy profile of local favorable sites and the excess ratio ($\chi = (d - d_{\text{perfect}})/d_{\text{perfect}}$) of interplanar spacing near the TB region as a function of the distance from TB. The sites with minimal formation energy are also shown in Fig. 6 (marked A, B, and C). The dashed line indicates the TB plane.

The $y$ axis of the simulation box for the case of TB ([110]/3), perpendicular to the twinning shear direction of hcp crystal and in the twinning plane, is the jump direction of He atom in bulk-Ti. The displacements (in the $\boldsymbol{y}$ direction) of Ti atoms in the TB region are very small. Therefore, the displacements have little effect on the configuration of the local favorable sites of He in this direction. It is found that the jump distance along the $y$ direction in the TB region is still $a$, consistent with that in bulk-Ti.

For comparison, the diffusion coefficients in the bulk Ti along the axes of the TB box are also computed through coordinate transformation. The matrix form of the diffusion coefficient ($\boldsymbol{D}'$) in the new coordinate system ($\boldsymbol{i'j'k'}$) can be obtained from $\boldsymbol{D}$ in the initial coordinate system ($\boldsymbol{ijk}$),

$$\boldsymbol{D}' = \boldsymbol{M} \cdot \boldsymbol{D} \cdot \boldsymbol{M}^{\mathrm{T}}, \tag{8}$$

where $\boldsymbol{M}$ is the transformation matrix ($(\boldsymbol{i'j'k'}) = (\boldsymbol{ijk})\boldsymbol{M}^{\mathrm{T}}$). At 600 K, according to the above formula, the calculated diffusion coefficient $5.98\times10^{-10}$ m$^2$/s in the $[1\bar{2}10]$ direction ($y$ axis) of bulk Ti is two orders of magnitude less than that in the TB region. However, the diffusion coefficients of the other two directions in bulk Ti are larger due to the contribution of the $\langle 0001 \rangle$ jump, which is different from the fact that the diffusion along the two directions in the TB region are slowed. As presented in Fig. 8, the relationship between the diffusion coefficient (along the $y$ axis) and temperature ($T$) is also explained by the Arrhenius law. Thus, the migration energy of a He atom along the $y$ axis in the TB region can be deduced from the slope of the curve. $\Delta E_{y,\text{TB}}$ is 0.083 eV and is less than that in bulk Ti (0.47 eV), i.e., there is little resistance for the jump of He atoms in the $y$ axis in the TB region. Therefore,

the He migration in the $y$ axis of the TB region is more rapid than that of the bulk.

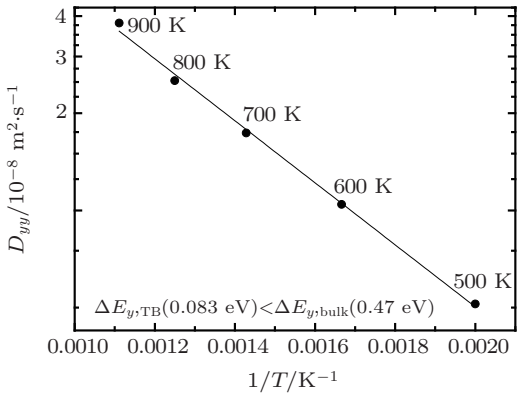



**Fig. 8.** Diffusion coefficient ($D$) along the $y$ axis of the TB box as a function of temperature ($T$) for He in the TB region. The migration energy ($\Delta E_y$) of a He atom along the $y$ axis in the TB region is less than that in bulk Ti.

Consistent with the case in the bulk Ti, $\mathrm{He}_n$ ($n = 2$, 3, and 4) atoms in the TB region migrate without dissociation. The ensemble averaged MSD $\langle R_y R_y \rangle$ along the $y$ direction at 600 K for $\mathrm{He}_2$ is also shown in Fig. 5. In accordance with the case of single He, the diffusion of $\mathrm{He}_2$ in the TB region is also anisotropic. However, the diffusion coefficient is less than that of single He. For $\mathrm{He}_3$ and $\mathrm{He}_4$, the diffusion is smaller. Thus, the MSDs are not plotted.

## 5. Conclusions

In this paper, we investigated the diffusion behavior of helium (He) in titanium (Ti) and the effect of grain boundary (GB) through molecular dynamics (MD) simulations. For the case of bulk Ti, diffusion of He is significantly anisotropic, and the diffusion coefficient of the [0001] direction is higher than that of the basal plane because the migration energy along the [0001] direction is less than that in the basal plane. It is determined that the most favorable interstitial site for He is the octahedral site and the jump behavior of He between these sites is different along different directions. The twin boundary (TB) was first constructed and relaxed with quenching MD. The relaxation of atomic configuration of the TB region will distort the local favorable site for He and affect its distribution. The TB region exhibits a high adsorption ability for the moving He atoms. TB accelerates the diffusion of He in the direction perpendicular to the twinning direction (TD) whereas it decelerates in the TD. This behavior is attributable to the change of diffusion path caused by the distortion of the local favorable site for He and the change of its number in the TB region.

## References


[1] Zhou X S, Liu Q, Zhang L, Peng S M, Long X G, Ding W, Cheng G J, Wang W D, Liang J H and Fu Y Q 2014 *In. J. Hydrogen Energ.* **39** 20062

[2] Zhou X S, Chen G J, Peng S M, Long X G, Liang J H and Fu Y Q 2014 *In. J. Hydrogen Energ.* **39** 11006

[3] Song Y M, Luo S Z, Long X G, An Z, Liu N, Pang H C, Wu X C, Yang B F and Zheng S X 2008 *Chin. Sci. Bull.* **53** 469

[4] Tanyeli I, Laurent M, Daniel M, Mauritius C M V D and Temmerman G D 2015 *Sci. Rep.* **5** 9779

[5] Li C, Greuner H, Yuan Y, Luo G N, Boswirth B, Fu B Q, Xu H Y, Jia Y Z and Liu W 2014 *J. Nucl. Mater.* **455** 201

[6] Wang J, Zhou Y L, Li M and Hou Q 2012 *J. Nucl. Mater.* **42** 7290

[7] Wang J, Hou Q, Sun T Y, Wu Z C, Long X G, Wu X C and Luo S Z 2006 *Chin. Phys. Lett.* **23** 1666

[8] Wang X S, Wu Z W and Hou Q 2015 *J. Nucl. Mater.* **465** 455

[9] Heung L K 1994 *Titanium for Long-Term Tritium Storage,* WSRD Report: WSRC-TR-94-0596

[10] Nishitani S R, Kawabe H and Aoki M 2001 *Mater. Sci. Eng. A-Struct.* **312** 77

[11] Fu B Q, Liu W and Li Z L 2009 *Appl. Surf. Sci.* **255** 9348

[12] Zhou X S, Long X G, Zhang L, Peng S M and Luo S Z 2010 *J. Nucl. Mater.* **396** 223

[13] Serra A and Bacon D J 1986 *Philos. Mag. A* **54** 793

[14] Wang L, Yang Y, Eisenlohr P, Bieler T R, Crimp M A and Mason D E 2010 *Metall. Mater. Trans. A* **41** 421

[15] Nie J F, Zhu Y M, Liu J Z and Fang X Y 2013 *Science* **340** 957

[16] Yu Q, Shan Z W, Li J, Huang X X, Xiao L, Sun J and Ma E 2010 *Nature* **463** 335

[17] Randle V, Rohrer G S and Hu Y 2008 *Scr. Mater.* **58** 183

[18] Bai X M, Voter A F, Hoagland R G, Nastasi M and Uberuaga B P 2010 *Science* **327** 1631

[19] Fu B Q, Lai W S, Yuan Y, Xu H Y and Liu W 2013 *Nucl. Instrum. Meth. B* **303** 4

[20] Fu B Q, Lai W S, Yuan Y, Xu H Y and Liu W 2012 *J. Nucl. Mater.* **427** 268

[21] Wang J, Hou Q, Sun T Y, Long X G, Wu X C and Luo S Z 2007 *J. Appl. Phys.* **102** 93510

[22] Chen M and Hou Q 2010 *Nucl. Sci. Tech.* **21** 271

[23] Chen M, Hou Q, Wang J, Sun T Y, Long X G and Luo S Z 2008 *Solid State Commun.* **148** 178

[24] Pasianot R and Savino E J 1992 *Phys. Rev. B* **45** 12704

[25] Zhou X W, Johnson R A and Wadley H N G 2004 *Phys. Rev. B* **69** 144113

[26] Zope R R and Mishin Y 2003 *Phys. Rev. B* **68** 24102

[27] Ackland G J 1992 *Philos. Mag. A* **66** 917

[28] Cleri F and Rosato V 1993 *Phys. Rev. B* **48** 22

[29] Kittel C 2005 *Introduction to Solid State Physics* (New York: John Wiley and Sons)

[30] Pearson W B 1958 *A Handbook of Lattice Spacings and Structures of Metals and Alloys* (Oxford: Pergamon)

[31] Wang J, Hirth J P and Tome C N 2009 *Acta Mater.* **57** 5521

[32] Young D A, Mcmahan A K and Ross M 1981 *Phys. Rev. B* **24** 5119

[33] Trinkaus H 1983 *Radiat. Eff.* **78** 189

[34] Cowgill D F 2005 *Fusion Sci. Technol.* **48** 539

[35] Zhang B L, Wang J, Li M and Hou Q 2013 *J. Nucl. Mater.* **438** 178

[36] Fu B Q, Xu B, Lai W S, Yuan Y, Xu H Y, Li C, Jia Y Z and Liu W 2013 *J. Nucl. Mater.* **441** 24

[37] Ziegler J F, Biersack J P and Littmark U 1985 *The Stopping and Range of Ions in Solid* (New York: Pergamon)

[38] Hou Q, Li M, Zhou Y L, Cui J C, Cui Z G and Wang J 2013 *Comput. Phys. Commun.* **184** 2091

[39] Swope W C, Andersen H C, Berens P H and Wilson K R 1982 *J. Chem. Phys.* **76** 637

[40] Legrand B, Treglia G, Desjonqueres M C and Spanjaard D 1986 *J. Phys. C-Solid State Phys.* **19** 4463

[41] Boisvert G and Lewis L J 1996 *Phys. Rev. B* **54** 2880

[42] Vincent-Aublant E, Delaye J M and Van Brutzel L 2009 *J. Nucl. Mater.* **392** 114

[43] Chandrasekhar S 1943 *Rev. Mod. Phys.* **5** 1

[44] Yelon A and Movaghar B 1990 *Phys. Rev. Lett.* **65** 618

[45] Wang Y L, Liu S, Rong L J and Wang Y M 2010 *J. Nucl. Mater.* **402** 55